Environmental Pollution 361 (2024) 124823

Contents lists available at ScienceDirect

Environmental Pollution

journal homepage: www.elsevier.com/locate/envpol

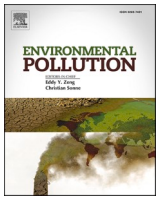

Divergent dual C-H isotopic fractionation pattern during anaerobic biodegradation of toluene within *Aromatoleum* species under nitrate-reducing conditions☆

Maria Pinel-Cabello [a], Kenneth Wasmund [b], Jesica M. Soder-Walz [a], Maria Vega [a], Mònica Rosell [c], Ernest Marco-Urrea [a,*]

[a] Departament d'Enginyeria Química, Biològica i Ambiental, Universitat Autònoma de Barcelona (UAB), Carrer de les Sitges s/n, Bellaterra, Spain
[b] School of Biological Sciences, University of Portsmouth, Portsmouth, UK
[c] Grup MAiMA, Mineralogia Aplicada, Geoquímica i Hidrogeologia (MAGH), Departament de Mineralogia, Petrologia i Geologia Aplicada, Facultat de Ciències de la Terra, Institut de Recerca de l'Aigua (IdRA), Universitat de Barcelona (UB), c/ Martí Franquès s/n, 08028, Barcelona, Spain

ARTICLE INFO

Keywords:
Aromatoleum
Toluene
Benzylsuccinate synthase
Isotope fractionation
Denitrifying bacteria

ABSTRACT

Toluene is a pollutant frequently detected in contaminated groundwater, mostly due to leakage from underground gasoline storage tanks and pipeline ruptures. Multi-element compound-specific isotope analysis provides a framework to understand transformation processes and design efficient remediation strategies. In this study, we enriched an anaerobic bacterial culture derived from a BTEX-contaminated aquifer that couples toluene and phenol oxidation with nitrate reduction and the concomitant production of carbon dioxide and biomass. The 16S rRNA gene amplicon data indicated that the toluene-degrading consortium was dominated by an *Aromatoleum* population (87 ± 2 % relative abundance), and metagenome sequencing confirmed that the genome of this *Aromatoleum* sp. encoded glycyl-radical enzyme benzylsuccinate synthase (BssABC) and phenylphospate synthase (PpsA1BC) homologous genes involved in the first step of toluene and phenol transformation, respectively. Carbon and hydrogen isotopic fractionation were $\varepsilon_{bulk,\ C} = -3.5 \pm 0.6$ ‰ and $\varepsilon_{rp,\ H} = -85 \pm 11$ ‰, respectively, leading to a dual C-H isotope slope of $\Lambda^{H/C} = 26 \pm 2$. This value fits with a previously reported value for a consortium dominated by an *Azoarcus* species ($\Lambda^{H/C} = 19 \pm 5$) but differs from that reported for *Aromatoleum aromaticum* ($\Lambda^{H/C} = 14 \pm 1$), both of which grow with toluene under nitrate-reducing conditions. Overall, this suggests the existence of different BssABC enzymes with different mechanistic motifs even within the same *Aromatoleum* genus.

1. Introduction

Toluene is a colorless volatile liquid and, together with benzene, ethylbenzene and xylene, forms an important group of aromatic volatile organic compounds called BTEX, which are major constituents of crude oil and fuel gasolines (Weelink et al., 2010). The most common sources of toluene into soils are from leaking underground storage tanks of BTEX-containing components such as gasoline, or from pipeline ruptures and waste disposal sites. Once released, it can be partially adsorbed on soil, and can also migrate down to the saturated zone by gravity and capillary forces, forming light non-aqueous phase liquids (LNAPLs) (Long et al., 2013). The leakage of BTEX poses a serious risk of groundwater contamination due to their relatively high solubility in water. According to the 2022 ATSDR Substance Priority List, toluene is ranked 75th (out of 275), based on a combination of frequency, toxicity and potential for human exposure. Repeated exposure to toluene has adverse effects on human health (such as a severe impact on the central nervous system) and, therefore, its removal from groundwater is an important environmental issue (Filley et al., 2004).

Bioremediation has promising applications in the BTEX contaminated groundwater. More specifically, enhancement of *in situ* biodegradation of toluene using microbial metabolism is considered a cost-effective, efficient, and less intrusive strategy than physicochemical methods (Bauer et al., 2008; Wartell et al., 2021). In the absence of

☆ This paper has been recommended for acceptance by Dr Yucheng Feng.

* Corresponding author.
E-mail address: Ernest.marco@uab.cat (E. Marco-Urrea).

https://doi.org/10.1016/j.envpol.2024.124823
Received 2 May 2024; Received in revised form 22 July 2024; Accepted 25 August 2024
Available online 26 August 2024

molecular oxygen (anoxic conditions), which is a frequent scenario in BTEX-contaminated soils, a broad variety of phylogenetically diverse bacteria have been demonstrated to degrade toluene using nitrate, sulfate, iron (III) or manganese (IV) as terminal electron acceptors (Atashgahi et al., 2021; Müller et al., 2009; Weelink et al., 2009). The initial step of anaerobic toluene catabolism is catalyzed by the enzyme benzylsuccinate synthase (BSS) that adds the methyl group of toluene to fumarate to yield *(R)*-benzylsuccinate (Fig. S1) (Biegert et al., 1996). This intermediate is further degraded by β-oxidation via a conserved specific pathway that consists of a benzylsuccinate CoA-transferase, benzylsuccinyl-CoA dehydrogenase and benzoylsuccinyl-CoA thiolase (Heider et al., 2016; Weiten et al., 2021). The enzymes required for benzylsuccinate formation and β-oxidation are encoded in two separate genetic units, namely the *bss* and *bbs* operons, respectively (Heider et al., 2016).

Bacterial members of the *Aromatoleum/Azoarcus/Thauera* cluster within the betaproteobacterial order Rhodocyclales encompass a group of model organisms to study anaerobic toluene degradation (Dorer et al., 2014; Tan and Parales, 2019; Weiten et al., 2021; Zhu et al., 2020). In particular, the genus *Aromatoleum* comprises a suite of 13 taxonomically described denitrifying species that degrade a wide variety of aromatic compounds under anoxic conditions. Species of this phylogenetic cluster are widely distributed in terrestrial and aquatic habitats, including agricultural soils, polluted sites and wastewater treatment plants, among others (Becker et al., 2022; Rabus et al., 2014).

A useful tool to investigate biological reactions of contaminants in the field, i.e., elucidate different degradation pathways and measure the efficacy of treatment systems, is compound-specific isotope analysis (CSIA). CSIA is a technique based on differences in reaction rates that take place between the heavy and light isotopes of an element that leads to a kinetic isotopic effect (KIE) in unidirectional reactions, due to differences in the activation energies between the heavy and light isotope in the bond (Dorer et al., 2016; Elsner et al., 2005). Thus, the reactant becomes enriched in the heavy isotope as the degradation reaction occurs for normal KIE (Elsner et al., 2005; Vogt et al., 2008). The extent of isotopic fractionation can be masked by processes that affect bond cleavage at the reaction site, e.g., substrate bioavailability, uptake, or binding to the enzyme, leading to differences in the observed isotope fractionation values (ε) and therefore apparent KIE for the same mechanism. In such cases, two-dimensional isotope fractionation analysis provides more precise information about the mechanism than a single isotope, by the correlation of isotope fractionation of two elements (Elsner, 2010; Vogt et al., 2008). Thus, a multidimensional isotope analysis is a key tool to identify the predominant degradation pathways of pollutants in the field. Dual C-H isotope analysis ($\Lambda^{H/C}$) of BTEX has been widely studied during biodegradation by different facultative and strictly anaerobic microorganisms, including *Aromatoleum* species, using several terminal electron acceptors (Dorer et al., 2016, 2014; Fischer et al., 2008; Vogt et al., 2008). In the case of toluene, differences in $\Lambda^{H/C}$ among different anaerobic bacteria degrading toluene by BSS ranged from 4 (anoxic phototrophic), 11–15 (nitrate-reducing conditions) to 24–31 (iron or sulfate-reducing conditions), suggesting the involvement of different isoenzymes of BSS under specific redox conditions (Kümmel et al., 2013; Dorer et al., 2016; Vogt et al., 2008).

The aim of this work is: i) to enrich and characterize a bacterial consortium obtained from a BTEX-contaminated aquifer that anaerobically degrades toluene, ii) to determine carbon and hydrogen isotope fractionation during toluene degradation under nitrate-reducing conditions to get more information on the reaction mechanism and iii) to obtain a draft genome assembly of the bacterium responsible for toluene degradation to identify target biodegradation genes.

2. Materials and methods

2.1. Inoculum source and enrichment of the toluene-degrading consortium

The toluene-degrading enriched culture obtained in this study derived from microcosms inoculated with a combination of groundwater and sediment samples collected from three sampling wells of a BTEX-contaminated aquifer located in the province of Barcelona (Spain). The samples were collected from the upper part of the aquifer (up to 10 m below ground surface) using a submersible stainless-steel pump. This upper part was an unconfined alluvial aquifer mainly composed of gravel layers of elevated hydraulic conductivity.

Unless otherwise stated, the culture was maintained in 100 mL glass bottles containing 65 mL of phosphate-buffered anaerobic medium modified from Ridgway et al. (1990) that contained KNO_3 (0.5 g/L), $(NH_4)_2SO_4$ (2.38 g/L), KH_2PO_4 (1.36 g/L), Na_2HPO_4 (1.42 g/L), $MgSO_4{\cdot}7H_2O$ (0.2 g/L), $ZnCl_2$ (0.07 mg/L), $CuSO_4{\cdot}5H_2O$ (0.039 mg/L), $FeSO_4{\cdot}7H_2O$ (5 mg/L), $CaCI_2{\cdot}2H_2O$ (10 mg/L), $MnSO_4{\cdot}H_20$ (1.54 mg/L), $Na_2MoO_4{\cdot}2H_2O$ (0.036 mg/L), $CoCl_2{\cdot}6H_20$ (0.19 mg/L), H_3BO_3 (2.86 mg/L) and nitrilotriacetic acid (NTA) (12.8 mg/L) as a chelating agent. The pH was adjusted to 7.2 with NaOH (1 M) prior to the addition of the trace metal solution. The serum bottles were sealed inside an anaerobic chamber (Coy Laboratory), with Teflon-coated butyl rubber stoppers and aluminium crimp caps. The cultures were amended with 1000 μM of neat toluene doses as a sole carbon source. The experimental bottles were then gassed with N_2 (0.4 bar overpressure) and incubated at 25 °C under static dark conditions to avoid possible photodegradation of toluene.

The consortium was maintained by transferring active cultures to fresh medium (2–5 % v/v) during the exponential degradation phase of toluene. Biotic (medium plus inoculum without toluene) and abiotic controls (medium amended with toluene but without inoculum) were included to evaluate the production of metabolites from the components of the medium and account for potential abiotic toluene degradation or volatile losses, respectively. All treatments were performed in triplicate. To ensure the equilibrium of gas-liquid phases in the microcosms, the initial concentration added at each toluene dose was measured the day after the addition. Given the high rate of toluene consumption by the consortium, the amount of toluene added to the abiotic controls was taken as the initial concentration.

2.2. Analytical methods

All BTEX were quantified by gas chromatography (GC) by injecting 0.5 mL of headspace gas samples into an Agilent 6890N GC equipped with a DB-624 column (30 m × 0.320 mm with 0.25 μm film thickness, Agilent) and a flame ionization detector (FID), using a gas-tight syringe (Hamilton). Helium was used as carrier gas. Injector and detector temperature was set at 250 °C and 300 °C respectively. The oven temperature was initially set isothermal at 45 °C. After sample injection, this temperature was held for 2 min and then ramped 10 °C/min up to 150 °C, when the rate increased to 20 °C/min to 220 °C. The running time was 16.3 min.

Phenol concentration was quantified with a Dionex Ultimate 3000 HPLC system equipped with a UV detector (272.6 nm) and a C18 reverse-phase column (Phenomenex, Kinetex EVO C18 100 Å, 5 μm, 4.6 mm × 250 mm). The mobile phase consisted of 30 % of acetonitrile and 70 % of MilliQ water with a constant flow of 1 mL/min.

Carbon dioxide was measured by injecting 0.1 mL of headspace gas sample into an Agilent 7802A GC equipped with a thermal conductivity detector (TCD) with MolSieve 5A 60–80 SS (1.82 m × 2 mm, Agilent) and a Porapak Q 60–80 UM columns (1.82 m × 2 mm, Agilent). Nitrogen was used as carrier gas. The initial oven temperature was fixed at 70 °C. After the injection of the sample, this temperature was held for 2 min and then declined at 20 °C/min to 40 °C, which was held for 4 min, with a total running time of 6 min. Injector and detector temperatures were

set at 200 °C and 250 °C, respectively.

Nitrate, nitrite, and sulfate were quantified from filtered liquid samples (0.22 μm) using a Dionex IC-2000 system with an IonPac AS11-HC-4 μm anion-exchange column (250 × 2 mm) and suppressed conductivity detection by a Dionex ASRS 300 in the AutiSuppression recycle mode. The column temperature was 30 °C. A sample volume of 2.5 μL was injected using a Dionex ASAP auto-sampler. The eluent was a KOH solution (30 mM) from a Dionex EGC 500 KOH cartridge. The analysis was performed isocratically with a flow rate of 0.38 mL/min.

All chromatographs used Chromeleon software (Thermo Scientific) for the calculation of peak areas. Aqueous standards were used for calibration under similar conditions as those in the microcosms (temperature, pressure, and liquid and headspace volumes). Results were presented as nominal concentrations.

For optical density (OD) determination, 1 mL of sample was collected, and the absorbance was measured using a Hach Lange DR 3900 spectrophotometer at a 600 nm wavelength.

2.3. Metagenomic sequencing and genomic analysis

For 16S rRNA gene amplicon sequencing and metagenome sequencing, cells were harvested by centrifugation (9000 *g*, 40 min at 16 °C; Avanti J-20 centrifuge) during the exponential degradation phase once the culture consumed ~1000 μM toluene, respectively.

DNA was extracted using Gentra Puregen Yeast/Bact Kit (Qiagen) according to the manufacturer's instructions. The DNA concentration (ng/μL) was determined by Nanodrop (Thermo Scientific-UV-Vis), using Hydratation Solution (1 μL) from Gentra Puregen Yeast/Bact Kit (Qiagen) as a blank.

Amplicons of the region V3-V4 of 16S rRNA genes were amplified with primers S-D-Bact-0341-b-S-17 (CCTACGGGNGGCWGCAG) and S-D-Bact-0785-a-A-21 (GACTACHVGGGTATCTAATCC) (Klindworth et al., 2013) and then sequenced with the Illumina MiSeq sequencing platform (2 x 250 bp) at *Serveis de Genòmica i Bioinformàtica* from *Universitat Autònoma de Barcelona* (Spain). Sequences were processed using the 16S Metagenomics workflow in the MiSeq Reporter analysis software based on quality scores generated by real-time analysis during the sequencing run. Quality-filtered indexed reads were demultiplexed for generation of individual FASTQ files and aligned using the banded Smith–Waterman method (Smith and Waterman, 1981) of the Illumina-curated version of the Greengenes taxonomic database. The output of this workflow was a classification of reads at multiple taxonomic levels.

Shotgun metagenomic sequencing of the DNA extracted from the cultures was also sequenced by the Illumina MiSeq sequencing platform (2 x 250 bp) at *Serveis de Genòmica i Bioinformàtica* from *Universitat Autònoma de Barcelona* (Spain). Sequence reads were trimmed of adapters using AdapterRemoval with default settings (Schubert et al., 2016), trimmed based on quality using a python3 script (https://github.com/kwasmund/Trim-Illumina), with the flags -q 15 -m 50 –b 8. Sequences were assembled using SPAdes (v. 3.9.0) with pre-assembly read-error correction (Bankevich et al., 2012). Contigs <2500 bp were discarded. Except for a contig containing ribosomal RNA genes, contigs that were more or less than 18–24 × coverage were also discarded, because BLASTX analyses against the National Center for Biotechnology Information (NCBI) nr database identified that contigs with this coverage all belonged to *Aromatoleum*.

The genome was annotated using the RAST server with 'classic mode' (Aziz et al., 2008) and MAGE MicroScope pipeline (Vallenet et al., 2020). The loci numbers used in this manuscript are from the MicroScope annotation and are preceded by the letters 'AROMA_V1_'. The JspeciesWS website (Richter et al., 2016) was used to calculate the average nucleotide identities (ANI) of genomes by BLASTn. Genome quality was evaluated with CheckM (Parks et al., 2015). The genome was classified using GTDB-tk (v2.3.2) with database version r214 (Chaumeil et al., 2020. The genome and annotations are publicly accessible in the MicroScope platform, accession WGS AROMA.1).

2.4. Stable carbon and hydrogen isotope experiments

Eight parallel experimental bottles were inoculated as described above and fed with 1000 μM toluene. Each bottle was killed at different extents of toluene degradation by adding 1 mL of concentrated HCl (37 %). Two types of controls were included in the experiment: i) abiotic controls, consisting of medium with toluene and without inoculum. These controls were added to consider the initial concentration of toluene spiked into the experimental bottles and potential abiotic reactions or contaminant losses, ii) killed controls, in which the inoculum was added and immediately killed with 1 mL of concentrated HCl, to evaluate the contribution of the residual toluene added with the inoculum on the isotopic composition.

Carbon and hydrogen isotopic composition of the toluene in the samples was measured at the *Centres Científics i Tecnològics de la Universitat de Barcelona* (CCiT-UB). The system consisted of a Thermo Finnigan Trace GC Ultra instrument coupled via a GC-Isolink interface to a Delta V Advantage IRMS (Thermo Fisher Scientific). Liquid aliquots were removed from the experimental bottles and placed in 20 mL vials filled with 10 mL aqueous phase (samples were diluted in Milli-Q water to reach a similar toluene concentration with a proper signal intensity) and containing a 30 mm PTFE-coated stir bar were placed in a TriPlus Autosampler equipped with a SPME holder (Thermo Fisher Scientific). The VOCs were extracted from the aqueous samples by automated headspace solid phase micro-extraction (HS-SPME) using a 75 μm Carboxen-PDMS fiber (Supelco, Bellefonte, PA, USA). Samples were extracted for 20 min at 40 °C and constant agitation and the SPME fiber was desorbed for 10 min at 250 °C at the GC injector set to split mode with a split ratio of 1:10. This GC was equipped with a Teknokroma TRB-624 column (60m × 0.32 mm x 1.8 μm, Barcelona, Spain). The oven temperature was kept at 60 °C for 2 min, heated to 220 °C at a rate of 8 °C min^{-1} and held at 220 °C for 5 min. Helium was used as a carrier gas (1.8 mL/min). The Quality Control/Quality Assurance (QC/QA) of the analytical process was carried out through the analysis of duplicate samples, blanks, and standards as shown below. For example, to correct slight isotopic fractionation induced by the HS-SPME preconcentration technique, the obtained delta values were corrected by daily values of calibrated in-house standards of known C and H isotope ratios (including the same pure toluene standard which was also used for the cultures), prepared at the same concentration range than the samples. These pure standards were previously determined using a Delta V elemental analyzer (EA) coupled to a Delta C IRMS through a Conflo IV interface (all parts of Thermo Fisher Scientific) for carbon and a Delta Plus XP IRMS with a high temperature conversion elemental analyzer (TC-EA) for hydrogen using several internal standards with known isotopic composition relative to the Vienna Pee Dee Belemnite (VPDB) standard and Vienna Standard Mean Ocean Water (VSMOW) respectively, according to (Coplen et al., 2006). All analyses (standards and experimental samples) were injected minimum in duplicate as a quality control and one standard deviation (1σ) was calculated. All the standards injected in different replicas, days and concentrations (from 50 to 2500 μg L^{-1}) had an average toluene-$\delta^{13}C$ values of −28 ± 0.2‰ (n = 17) and $\delta^{2}H$ values of −58.8 ± 4.5‰ (n = 20), which associated errors are smaller than the typical total analytical uncertainty (0.5‰ for carbon and 5‰ for hydrogen).

Carbon isotopic fractionation accounting for all atoms ($\varepsilon_{bulk,\ C}$) was calculated according to the simplified logarithmic Rayleigh equation (Eq. (1)) (Dorer et al., 2016):

$$ln\left(\frac{\delta_t + 1}{\delta_0 + 1}\right) = \varepsilon_{bulk} * ln\left(\frac{C_t}{C_0}\right) \quad \text{Eq. (1)}$$

where δ is the relative difference of isotope ratios expressed in per mil (initial subscript 0 and *t* at each degradation point measured). *C*

represents the initial toluene concentration (0) and at each measuring point during the experiment (*t*). ε in the equation is the corresponding isotopic fractionation.

For hydrogen, corrected isotope fractionation in the reactive positions ($\varepsilon_{rp,\ H}$) (Eq. (2)) was calculated, as $|\Delta\delta^2H = \delta_{t,H} - \delta_{0,H}|$ exceed 100 ‰ and compared to normal $\varepsilon_{bulk,\ H}$ which might not be consistent for high hydrogen fractionation. Thus, $\varepsilon_{rp,\ H}$ allows to obtain stable isotopic factors regardless of the extent of hydrogen fractionation (Dorer et al., 2016):

$$ln\left(\frac{\left(\delta_t + \frac{n}{x}\left(\delta_t - \delta_0\right) + 1\right)}{\delta_0 + 1}\right) = \varepsilon_{rp} * ln\left(\frac{C_t}{C_0}\right) \quad \text{Eq. (2)}$$

The Eq. (2) considers the atoms that are in the reactive position (subscript *rp*), where *n* is the number of atoms of an element in the molecule, and *x* the total number of an element in the reactive site. Confidence interval of 95% (95% CI) of the linear regression in the Rayleigh plots was estimated for ε values.

To evaluate the isotope effect of the atoms at the reactive position of the molecule, the apparent kinetic isotope effect (AKIE) was calculated as follow in Eq. (3), where *n* represents the total number of atoms of the considered element (E) in the target molecule, *x* denotes the number of atoms situated at the reactive site, and *z* stands for the number of atoms in intramolecular isotopic competition (Elsner et al., 2005).

$$AKIE_E = \frac{1}{1 + \left(\frac{n \bullet z}{x} \bullet \varepsilon bulk\right)} \quad \text{Eq. (3)}$$

Dual isotope slopes ($\Lambda^{H/C}$) were calculated by ordinary linear regression of the changes in δ^2H and $\delta^{13}C$ data in 2D-isotope plots (i.e., $\Lambda^{H/C} = \Delta\delta^2H/\Delta\delta^{13}C$). The uncertainty of $\Lambda^{H/C}$ was reported as the 95% CI, determining the uncertainty of $\Delta\delta$ values by error propagation. To get further mechanistic insights, obtained $\Lambda^{H/C}$ values were compared to the theoretical one estimated by Eq. (4), which expresses the dual isotope slope for a given substrate and reaction as a function of KIE values (Elsner, 2010). Both equations (3) and (4) assume the absence of secondary isotope effects. For carbon, secondary isotope effects are usually insignificant.

$$\Lambda^{H/C} = \frac{\Delta\delta^2H}{\Delta\delta^{13}C} \approx \frac{\varepsilon^H_{bulk}}{\varepsilon^C_{bulk}} \approx \frac{\left(\frac{x}{n}\right)_H}{\left(\frac{x}{n}\right)_C} \bullet \frac{AKIE_H - 1}{AAKIE_C - 1} \bullet \frac{1 + AKIE_H \bullet (z_H - 1)}{1 + AKIE_C \bullet (z_C - 1)} \quad \text{Eq. (4)}$$

Statistical differences with previously reported values were assessed using statistical two-tailed z-score tests (Ojeda et al., 2019). Differences were considered statistically significant if $p \leq 0.05$.

3. Results and discussion

3.1. Enrichment and characterization of the toluene-degrading consortium

A combination of groundwater and sediments from an aquifer contaminated with BTEX were incubated with the anoxic buffered medium amended with toluene. In the first transfer, 1000 μM of toluene was consumed within a week. After the tenth consecutive transfer, we explored which electron acceptor was used for toluene oxidation. We replaced the sulfate salts of the buffered solution with chloride salts (1.3 g NH_4Cl, 0.2 g/L $MgCl_2{\cdot}6H_2O$, 5 mg/l $FeCl_2{\cdot}4H_2O$, 1.54 mg/L $MnCl_2{\cdot}4H_2O$ and 0.039 mg/L $CuCl_2{\cdot}2H_2O$) and increasing the concentration of KNO_3 to 1.01 g/L to evaluate whether nitrate was used as electron acceptor and not sulfate. Similarly, to assess whether sulfate acted as electron acceptor, the only nitrate source in the medium (KNO_3) was replaced with a sulfate salt (2.38 g/L $(NH_4)_2SO_4$). Toluene was completely degraded within six days in the medium that contained nitrate as electron acceptor, whereas toluene was not consumed in the medium containing sulfate after 40 days of incubation (Fig. S2). Thus, the medium containing nitrate as electron acceptor was selected for further studies.

After fifteen consecutive transfers in the medium containing nitrate as electron acceptor, a time-course experiment to evaluate degradation of toluene was performed. Toluene degradation was concomitant to nitrate consumption, indicating that it was used as terminal electron acceptor (Fig. 1A and B). The transient accumulation of nitrite, an obligate intermediate of all nitrate reduction pathways, together with the overpressure observed during sampling in the bottles consuming

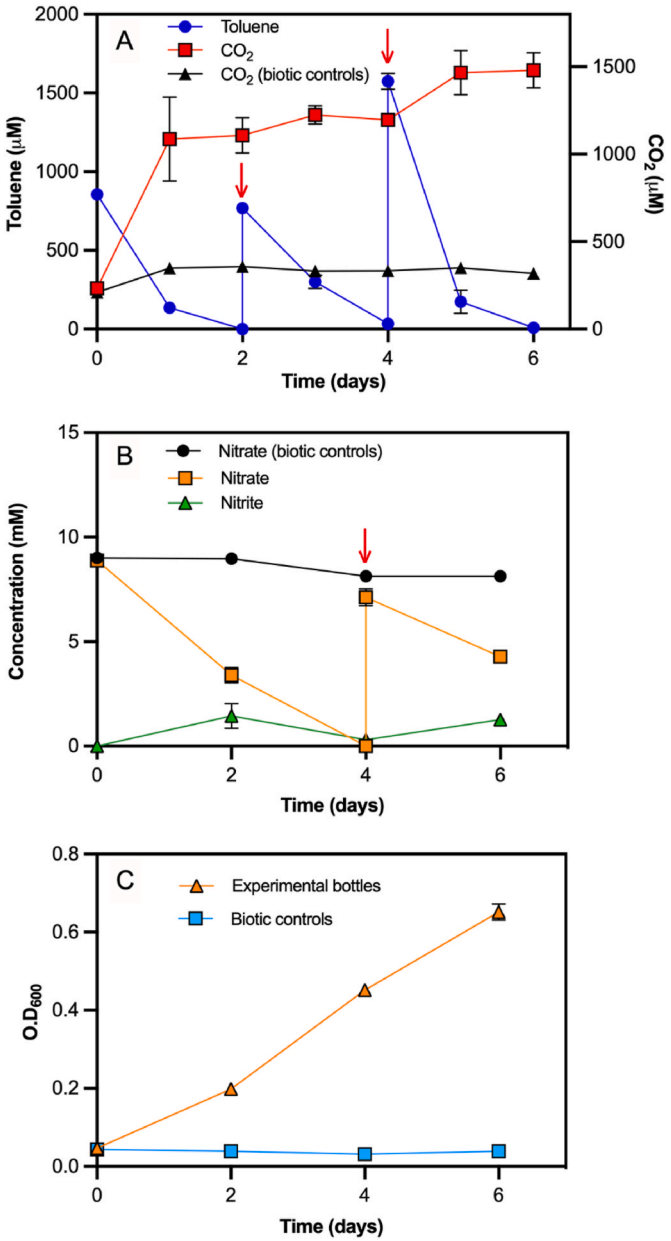

Fig. 1. (A) Time course of toluene degradation and CO_2 production in experimental bottles and biotic controls. (B) Nitrate concentration in experimental bottles and abiotic controls and nitrite concentration in experimental bottles. (C) $O.D_{600}$ in experimental bottles and biotic controls. Red arrows in panel A and B indicate the re-amendment of toluene and nitrate, respectively. This experiment was performed with triplicate cultures growing on toluene after 15 transfers with the medium containing nitrate as terminal electron acceptor. (For interpretation of the references to color in this figure legend, the reader is referred to the Web version of this article.)

toluene, further suggests that nitrate was reduced to nitrogen gas. However, further studies are required to confirm complete denitrification. The concentration of nitrate in both biotic and abiotic controls remained constant at 8.12 ± 0.08 and 8.7 ± 0.6 mM, respectively, which confirms biological oxidation of toluene coupled to nitrate reduction in the experimental bottles. After the consumption of the second dose of toluene (day 4), nitrate was reamended to proceed with toluene oxidation.

Carbon dioxide was concomitantly produced when toluene was oxidized (Fig. 1A). The amount of CO_2 detected in biotic controls remained low (with an average of 357 ± 56 mM), which could be attributed to the oxidation of residual toluene added when inoculating the culture medium. Similarly, consumption of toluene was accompanied by a clear increase in the optical density at 600 nm of the medium, suggesting that metabolism of toluene was coupled to growth (Fig. 1C).

The stoichiometry of toluene oxidation relative to nitrate consumption in the experimental bottles (C_7H_8:NO_3^-) was 1:4.3 ± 2.3 (Table 1), which fits well with the stoichiometric ratio of 1:4.5 reported by Evans et al. (1991) during toluene degradation by a denitrifying enriched culture (Eq. (5)):

$$C_7H_8 + 4.5NO_3^- + 4.5H^+ + 0.68NH_3 \rightarrow 3.6CO_2 + 0.68C_5H_7O_2N + 2.25N_2 + 4.9H_2O \quad \text{(Eq. 5)}$$

In the case of stoichiometry of toluene oxidation relative to carbon dioxide production (C_7H_8:CO_2), an experimental ratio of 1:0.4 ± 0.4 was obtained, which corresponds to only around 8% of the molar ratio represented in Eq. (5) (1:3.6). It can be explained by the solubilization of CO_2 to HCO_3^- to equilibrate the charge balance due to the transformation of NO_3^- to N_2, that would contribute to the alkalinity of the medium (Eq. (6)). Notable CO_2 production was observed over the time course experiment, especially during the consumption of the first dose of toluene.

$$C_7H_8 + 4.5NO_3^- + 0.9H^+ + 0.68NH_3 \rightarrow 3.6HCO_3^- + 0.68C_5H_7O_2N + 2.25N_2 + 1.3H_2O \quad \text{(Eq. 6)}$$

3.2. Alternative carbon sources of the toluene-degrading culture

The potential of the *Aromatoleum*-containing consortium to use other contaminants as carbon sources was assessed under nitrate-reducing conditions by replacing toluene in the culture medium with different substrates that were previously tested for *Aromatoleum* species by Rabus et al. (2019): benzene, ethylbenzene, xylene isomers (*ortho*-, *para*-, and *meta*-xylene), limonene, propylbenzene, benzoate and phenol (Table S1).

Among all the substrates tested, phenol was the most favourable carbon source, and the culture consumed doses of ~500 μM in less than two days with the concomitant production of CO_2 (Fig. S3A). Furthermore, as observed in the case of toluene, when phenol was consumed nitrate was consumed with a low accumulation of nitrite (Fig. S3B), and the increase in the optical density over time indicated that phenol was partially assimilated to generate new biomass (Fig. S3C).

In order to determine if there was a preference for the consumption of toluene or phenol by the consortium, both contaminants were added simultaneously to the culture medium. Toluene and phenol were consumed concomitantly within two days without an observable lag phase and were accompanied by a large increase in the optical density (Fig. S4).

3.3. Microbial composition of the consortium and metagenome sequencing of the toluene-degrading bacterium

Amplicon sequencing of 16S rRNA genes was carried out to determine the bacterial community of the toluene-degrading consortium. The results showed that the predominant genus was Aromatoleum (87 ± 2 %), followed by Stenotrophomonas (3 ± 0.1 %), Proteiniphilum (3 ± 1 %), Simpliscispira (2 ± 0.4 %), Paludibacter (2 ± 0.6 %), and others (Fig. 2). This "others" category includes unclassified reads at genus level (0.8 ± 0.2 %), Alicycliphilus (0.6 ± 0.01 %) and Pseudomonas (0.4 ± 0.1 %) (Fig. 2).

Of the detected genera, *Aromatoleum* was the most abundant bacterial genus, and widely known for the ability of members of this genus to transform toluene under nitrate-reducing conditions. Some species of *Pseudomonas* are also able to degrade toluene under nitrate-reducing conditions (Banerjee et al., 2022; Kim et al., 2013; Rajamanickam et al., 2017), although the very low relative abundance of this group in the culture (0.4 ± 0.1 %) suggests that either these *Pseudomonas* do not use toluene as carbon source or its contribution to the overall degradation is negligible. Therefore, we assume that *Aromatoleum* sp. are responsible for toluene degradation in our culture.

Regarding other bacteria detected in our consortium, *Alicycliphilus denitrificans* strains BC and K601 oxidize benzene and toluene, but using chlorate as terminal electron acceptor (Oosterkamp et al., 2013; Solís-González and Loza-Tavera, 2019). A species of *Stenotrophomonas* can grow with benzene, trichloroethylene and chloroform, but growth with toluene was barely observed and it did not grow with phenol (Mukherjee and Roy, 2013). *Proteiniphilum* has also been detected in diverse cultures degrading polycyclic aromatic hydrocarbons and its role is commonly attributed to proteolytic fermentation, yielding acetate and propionate as products (Chen and Dong, 2005). Hence, this genus, along with other fermenters such as *Paludibacter,* might be the main degraders of proteins from the cell debris in the culture (Müller et al., 2009; Ueki et al., 2006).

The draft genome of the *Aromatoleum* sp. in the culture consisted of 5,073,668 bp in 50 contigs with a G + C content of 66.2%. The genome was estimated to be 99.9% complete from CheckM analysis, with 0.7% contamination. This suggests that the genome of the *Aromatoleum* strain from our consortium is near-complete. The genome was classified as an unidentified species of the genus *Aromatoleum* by GTDB-tk. Analysis of average nucleotide identity (ANI) similarity to other available *Aromatoleum* genomes showed it had 83.5% ANI to the next closest species. This also suggests the genome should be considered representative of a novel species-level genome considering a >95% ANI threshold to define species (Jain et al., 2018). The closest species based on ANI were *Aromatoleum buckelii* (GCF_012910785) and *Aromatoleum bremense* (GCF_017894365), both with 83.5% ANI.

In agreement with the biodegradability tests performed in section 3.2, the genes encoding enyzmes involved in the initial steps of toluene, phenol and benzoate degradation were encoded in the genome of the *Aromatoleum* sp. in the culture. These were: the glycyl-radical enzyme benzylsuccinate synthase (BssABC) that adds toluene to the double bond of the fumarate cosubstrate forming *(R)*-benzylsuccinate; the

Table 1
Average degradation rate and balances of CO_2 produced, and nitrate consumed per toluene dose for the experiment depicted in Fig. 1. The stoichiometric balances were calculated according to Eq. (5). The CO_2 stoichiometrically produced was calculated as the average of the CO_2 produced during the three toluene doses.

Days	Toluene consumed (mM)	Degradation rate (mmol d^{-1} L^{-1})	CO_2 produced (mM)	Ratio C_7H_8:CO_2	Nitrate consumed (mM)	Ratio C_7H_8:NO_3^-
2	0.8538 ± 0.0007	0.4 ± 0.4	0.7 ± 0.1	3.074 ± 0.003	5.6 ± 0.4	3.842 ± 0.003
4	0.74 ± 0.03	0.37 ± 0.01	0.11 ± 0.02	2.65 ± 0.09	3.4 ± 0.4	3.3 ± 0.1
6	1.566 ± 0.004	0.783 ± 0.002	0.3 ± 0.1	5.64 ± 0.02	2.8 ± 0.2	7.05 ± 0.02

homologous genes encoding the phenylphospate synthase (PpsA1BC) that transforms phenol to phenylphosphate; and the ATP-dependent benzoate-CoA ligase that activates benzoate to benzoyl-CoA (Table S2).

3.4. C and H isotopic fractionation during anaerobic degradation of toluene

The carbon and hydrogen isotope fractionation of toluene produced by the denitrifying enriched culture was determined to provide insights into its degradation mechanisms.

Toluene degradation was accompanied by a significant enrichment of ^{13}C and ^{2}H in its residual fraction with respect to the abiotic controls, increasing from −27.8 ± 0.2 ‰ and −67.2 ± 1.9 ‰ to −18.751 ± 0.003 ‰ and +166.9 ± 0.1 ‰, respectively. The corresponding isotopic fractionation for each element calculated with the Rayleigh equation were $\varepsilon_{bulk,\ C} = -3.3 \pm 0.9$ ‰ and $\varepsilon_{bulk,\ H} = -85 \pm 11$ ‰, showing in both cases good correlation between toluene concentration and isotope signatures ($R^2 = 0.97$ and 0.98, respectively) (Fig. 3A and B).

The carbon isotopic fractionation obtained in our study is statistically different from that obtained previously during toluene oxidation by other nitrate-reducing bacteria ($p < 0.05$), except for *Aromatoleum aromaticum* EbN1 ($\varepsilon_{bulk,\ C}$ of −3.8 ± 0.5 ‰, $p > 0.05$, Table 2) (Dorer et al., 2016; Vogt et al., 2008). Interestingly, the hydrogen isotopic fractionation obtained ($\varepsilon_{bulk,\ H}$ of −85 ± 11 ‰) is significantly higher ($p < 0.001$) than that calculated for *T. aromatica* (−51 ± 9 ‰), and *A. aromaticum* EbN1 (−45 ± 15 and −58 ± 10 ‰), but it is within the range described for *Azoarcus* T (Table 2) (Dorer et al., 2016; Vogt et al., 2008). These values vary notably among other denitrifying bacteria that oxidize toluene. In fact, toluene biodegradation shows a high variability among bacteria with the same presumed catabolic mechanism (fumarate addition), as observed with the strains belonging to the phylogenetic cluster *Aromatoleum/Azoarcus/Thauera*. For instance, $\varepsilon_{bulk,\ C}$ of toluene in *T. aromatica* ranges from −2.7 to −1.7 ‰ and higher values were observed for *Azoarcus* sp. strain T, ranging from +5.6 to +6.2 ‰ (Meckenstock et al., 1999; Vogt et al., 2008). Similarly, $\varepsilon_{bulk,\ H}$ ranges from −35 ± 14 to −79 ± 21 ‰ in *T. aromatica* and *Azoarcus* T, respectively (Meckenstock et al., 1999; Vogt et al., 2008) (Table 2).

Given the extent of $\Delta\delta^2H$ (up to +234‰), Eq. (2) (section 2.4) was applied considering the methyl moiety attack for adding the fumarate, affecting 3 ($x = 3$) out of 8 atoms ($n = 8$) of hydrogen at the reactive position (Dorer et al., 2014). The $\varepsilon_{rp,\ H}$ obtained was −197 ± 28 ‰, considerably higher than the $\varepsilon_{bulk,\ H}$. However, the linearity of our data was not improved by the application of this correction ($R^2 = 0.98$, Fig. 2B and C), probably because only two $\Delta\delta^2H$ values (out of 9) exceeded 100 ‰, and therefore both calculations provide robust

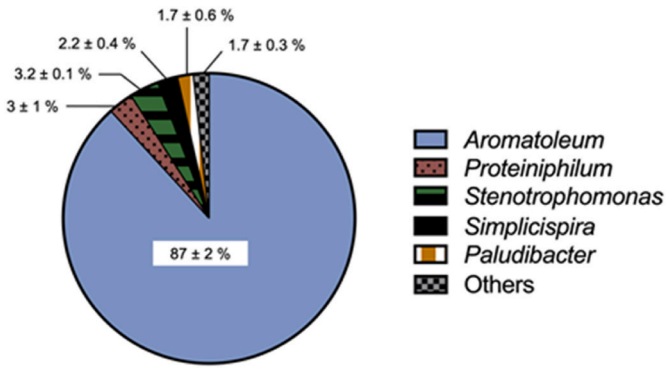

Fig. 2. Relative abundance of bacterial taxa in the toluene-degrading culture after Illumina sequencing of the 16S rDNA. This graph was drawn with the average of triplicate microcosms with corresponding standard deviations. The cultures used in this experiment were grown with the medium containing nitrate as terminal electron acceptor for six consecutive transfers.

hydrogen isotopic fractionation factors. Either way, similar conclusions can be drawn from the comparison of the $\varepsilon_{rp,\ H,}$ showing high variability among strains (Table 2), reaching even −607 ± 88 ‰ in studies combining labeled and non-labeled toluene with *T. aromatica* (Elsner et al., 2005; Meckenstock et al., 1999).

AKIEs were calculated using Eq. (3) assuming toluene oxidation by fumarate addition to the methyl group as reaction mechanism. Apparent kinetic isotopic effect obtained for carbon ($AKIE_C$) with 7, 1, and 1 as n/x/z values was 1.024 ± 0.004, which agrees surprisingly well with the maximum estimations of Streitweiser semiclassical limit for KIE in C-H bonds (1.021) (Huskey, 1991), because realistic values with transition states at about 50% bond cleavage can be expected to be half as pronounced (1.01) (Elsner et al., 2005). However, in the case of hydrogen, the corresponding $AKIE_H$ calculated with n/x/z values of 8, 3, and 3 was 2.45 ± 0.04, lower than the expected theoretical value (6.4). Both AKIEs are in any case in the range previously observed in the literature for toluene-degrading nitrate-reducing bacteria, as already mentioned for the epsilon values. Vogt et al. (2008) reported AKIEs that ranged between 1.019-1.026 and 1.5–1.7 for carbon and hydrogen respectively, in *A. aromaticum* EbN1. Similarly, AKIEs described for the consortium dominated by *Azoarcus* DD-Anox1 were among 1.020–1.026 for carbon and 1.9–2.2 for hydrogen fractionation (Dorer et al., 2016).

Correlation of the obtained carbon and hydrogen isotope fractionation values fits well to linear regression ($R^2 = 0.995$), with a slope of $\Lambda^{H/C} = 26 \pm 2$ and even better with $\zeta^*(rp)^{H/C} = 20.9 \pm 0.8$ ($R^2 = 0.998$) (Fig. 4A and B respectively). The $\Lambda^{H/C}$ found is also in agreement with

Table 2
Comparison of different isotopic parameters of *Aromatoleum* sp with other nitrate-reducing bacteria using the benzylsuccinate synthase pathway for toluene degradation. Asterisks indicate statistically significant differences from the values obtained in this study.

Parameter	*Aromatoleum* sp. (this study)	*A. aromaticum* EbN1[a]	DD-Anox1[b]	*Azoarcus* T[a]	*T. aromatica*[a]	*G. toluolica*[b]
$\varepsilon_{bulk,\ C}$	−3.5 ± 0.6	−3 ± 0.1* −3.8 ± 0.5	−2.4 ± 0.4***	−5.6 ± 0.3*** −6.2 ± 1.1***	−2.7 ± 0.1 −2.4 ± 0.6 −1.7 ± 0.1	−2.6 ± 0.1
$\varepsilon_{bulk,\ H}$	−85 ± 11	−45 ± 15*** −58 ± 10***	−73 ± 9	−79 ± 7 −79 ± 21	−35 ± 14 −51 ± 9***	−58 ± 4
$\varepsilon_{rp,\ H}$	−197 ± 28	−110 ± 41*** −145 ± 23***	−171 ± 10	−187 ± 24 −195 ± 46	−88 ± 35 −126 ± 23***	−142 ± 7
$\Lambda^{H/C}$	26 ± 2	14 ± 4*** 14 ± 1***	19 ± 5***	15 ± 2*** 11 ± 2***	11 ± 5 20 ± 6	23 ± 2
$\zeta^*(rp)^{H/C}$	20.9 ± 0.8	14 ± 2***	20 ± 2	–	–	21 ± 2
$AKIE_C$	1.024 ± 0.004	1.023 ± 0.004	1.023 ± 0.003	1.038 ± 0.001 1.044 ± 0.008	1.019 ± 0.001 1.0157 1.012 ± 0.001	1.018 ± 0.001
$AKIE_H$	2.45 ± 0.04	1.6 ± 0.1	2.1 ± 0.2	2.2 ± 0.4 2.4 ± 0.8	1.4 ± 0.2 1.6077	1.7 ± 0.1

[a] Vogt et al. (2008).
[b] Dorer et al. (2016).

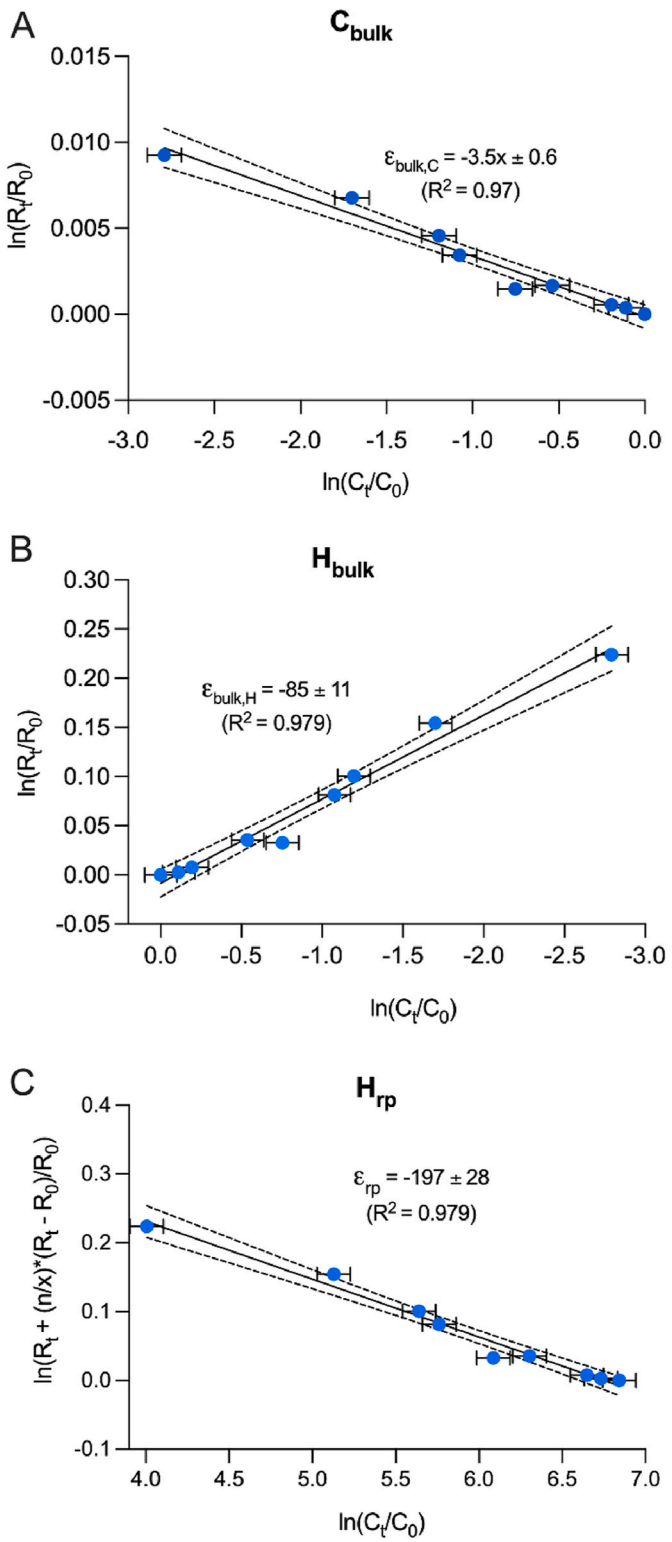

Fig. 3. Double logarithmic Rayleigh plots of $\Delta\delta^{13}C$ (A) and $\Delta\delta^{2}H$ (B), and H_{rp} (C) for toluene degradation by the mixed culture under nitrate-reducing conditions. The error bars represented the uncertainty calculated by error propagation including uncertainties in concentration and isotope measurements. In some cases, error bars are smaller than the symbols. Dashed lines indicate 95% confidence intervals.

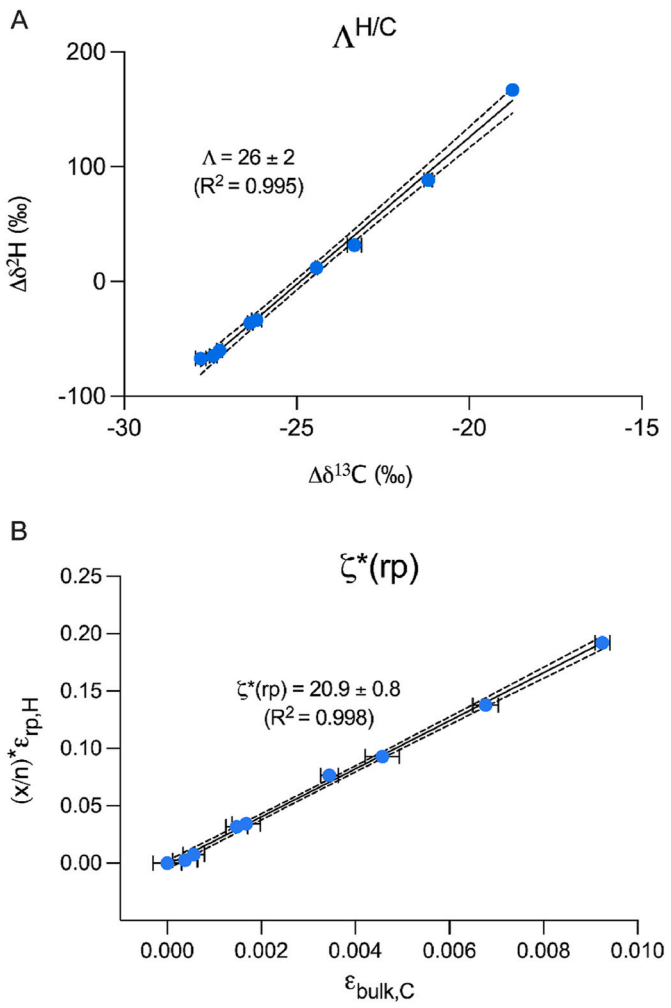

Fig. 4. Dual isotope plot of $\Delta\delta^{2}H$ vs $\Delta\delta^{13}C$ (A) and calculated $\zeta^{*}(rp)^{H/C}$ (B) during toluene degradation by the mixed culture under nitrate-reducing conditions. In some cases, error bars are smaller than the symbols. Dashed lines indicate 95 % confidence intervals.

the theoretical one for the oxidation mechanism as deduced from the obtained AKIE values using Eq. (4) ($\Lambda^{H/C}$ = 26.8). In line with the variations in isotopic fractionation values, especially for hydrogen, dual element plots $\Lambda^{H/C}$ and $\zeta^{*}(rp)^{H/C}$ showed significant differences to that reported for a nitrate-reducing, toluene-degrading enrichment cultures (DD-Anox1) dominated by an *Azoarcus* species ($\Lambda^{H/C}$ = 19 ± 5 (p < 0.05)), *Azoarcus* T ($\Lambda^{H/C}$ = 11 ± 2 and 15 ± 2 (p < 0.001)), and *A. aromaticum* ($\Lambda^{H/C}$ = 14 ± 4, $\zeta^{*}(rp)^{H/C}$ = 14 ± 2 (p < 0.001)) (Table 2) (Dorer et al., 2016; Vogt et al., 2008). In a previous study, it was proposed that the differences observed in the $\Lambda^{H/C}$ values between obligate and facultative toluene-degrading bacteria were associated with the phylogeny of *bssA* genes and therefore amino acid differences, which might lead to slightly different reactions paths (Kümmel et al., 2013). Differences at the amino acid level within the active sites of BssA might potentially produce the wide range of $\Lambda^{H/C}$ values observed.

3.5. Environmental implication

Toluene is a contaminant of great concern frequently found in groundwater from spills of solvent and petroleum products, or leaks from underground storage tanks. In this study, we showed a significant carbon and hydrogen fractionation of toluene during its anaerobic degradation by an *Aromatoleum*-enriched consortium. The higher fractionation values of the enriched consortium, especially for hydrogen, in

contrast to other nitrate-reducing toluene-degrading cultures, would make it more easily detected even at lower biodegradation rates, becoming useful as an indicator of natural attenuation in contaminated environments or a promising candidate for bioaugmentation treatments.

Although the dual isotope fractionation pattern obtained in this study ($\Lambda^{H/C}$ and $\zeta^{*}(rp)^{H/C}$) are much higher than *A. aromaticum* EbN1 and other close-related species ($p < 0.05$) (Dorer et al., 2016; Vogt et al., 2008), it still permits to distinguish between toluene oxidation by *Aromatoleum* sp. cultivated under nitrate-reducing conditions and *in-situ* chemical oxidation (ISCO) treatments in field studies. Despite the variability observed in $\varepsilon_{bulk,C}$ and $\varepsilon_{bulk,H}$ values depending on the chemical oxidation reaction, the slopes of $\Lambda^{H/C}$ were very similar, being 35 ± 10, 34 ± 2 and 34 ± 6 for persulfate, UV/H_2O_2 and permanganate respectively (Solano et al., 2018; Wijker et al., 2013; Zhang et al., 2016). Therefore, the isotopic fractionation patterns of toluene abiotic chemical oxidation differ from that detected for our enriched culture ($\Lambda^{H/C} = 26 \pm 2$), allowing to efficiently distinguish it from typical ISCO treatments eventually used in a field site.

4. Conclusions

In this study, we enriched a culture obtained from BTEX-contaminated groundwater under nitrate-reducing conditions that oxidizes toluene. The mixed culture consumed doses of 1000 μM toluene within two days, with the concomitant production of CO_2 and biomass. The ratio between nitrate consumption and toluene degradation was nearly stoichiometric. In addition to toluene, phenol was also oxidized under nitrate-reducing conditions with the concomitant production of CO_2 and biomass. The characterization of the microbial community revealed that an *Aromatoleum* sp. was the predominant bacterium in the culture (87 ± 2 % of relative abundance), which was assumed to have a role on toluene oxidation because this genus is well known for its capability to degrade aromatic compounds. Phylogenetic analyses of the 16S rRNA genes also showed that this strain is closely related to the genera cluster of *Aromatoleum/Azoarcus/Thauera*, being most closely related to *Aromatoleum* spp. The values of C and H isotope fractionation during toluene oxidation obtained in this study are valuable information that can be used to distinguish and quantify the degree of *in situ* biodegradation of this pollutant in the field.

CRediT authorship contribution statement

Maria Pinel-Cabello: Writing – original draft, Visualization, Investigation. **Kenneth Wasmund:** Writing – review & editing, Formal analysis, Data curation. **Jesica M. Soder-Walz:** Writing – review & editing, Supervision, Methodology. **Maria Vega:** Writing – review & editing, Methodology, Investigation. **Mònica Rosell:** Writing – review & editing, Supervision, Methodology. **Ernest Marco-Urrea:** Writing – review & editing, Supervision, Funding acquisition, Conceptualization.

Declaration of competing interest

The authors declare that they have no known competing financial interests or personal relationships that could have appeared to influence the work reported in this paper.

Data availability

Data will be made available on request.

Acknowledgments

This work was supported by the Spanish Ministry of Science and Innovation (projects PID2022-138929OB-I00, CTM2016-75587-C2-1-R and PID2019-103989RB-100) and the Generalitat de Catalunya (Consolidate Research Group 2021-SGR-01008 and 2021 SGR 00308). M.P. acknowledges a Margarita Salas postdoctoral fellowship from Ministerio de Universidades (MS2021-88). We thank CCiT-UB for the technical support.

Appendix A. Supplementary data

Supplementary data to this article can be found online at https://doi.org/10.1016/j.envpol.2024.124823.

References

Atashgahi, S., Oosterkamp, M.J., Peng, P., Frank, J., Kraft, B., Hornung, B., Schleheck, D., Lücker, S., Jetten, M.S.M., Stams, A.J.M., Smidt, H., 2021. Proteogenomic analysis of Georgfuchsia toluolica revealed unexpected concurrent aerobic and anaerobic toluene degradation. Environmental Microbiology Reports 13, 841–851. https://doi.org/10.1111/1758-2229.12996.

Aziz, R.K., Bartels, D., Best, A.A., DeJongh, M., Disz, T., Edwards, R.A., et al., 2008. The RAST server: rapid annotations using subsystems technology. BMC Genom. 9, 75. https://doi.org/10.1186/1471-2164-9-75.

Banerjee, S., Bedics, A., Tóth, E., Kriszt, B., Soares, A.R., Bóka, K., Táncsics, A., 2022. Isolation of Pseudomonas aromaticivorans sp. nov from a hydrocarbon-contaminated groundwater capable of degrading benzene-, toluene-, m- and p-xylene under microaerobic conditions. Front. Microbiol. 13.

Bankevich, A., Nurk, S., Antipov, D., Gurevich, A.A., Dvorkin, M., Kulikov, A.S., et al., 2012. SPAdes: a new genome assembly algorithm and its applications to single-cell sequencing. J. Comput. Biol. 19, 455–477. https://doi.org/10.1089/cmb.2012.0021.

Bauer, R.D., Maloszewski, P., Zhang, Y., Meckenstock, R.U., Griebler, C., 2008. Mixing-controlled biodegradation in a toluene plume — results from two-dimensional laboratory experiments. J. Contam. Hydrol. 96, 150–168. https://doi.org/10.1016/j.jconhyd.2007.10.008.

Becker, P., Döhmann, A., Wöhlbrand, L., Thies, D., Hinrichs, C., Buschen, R., Wünsch, D., Neumann-Schaal, M., Schomburg, D., Winklhofer, M., Reinhardt, R., Rabus, R., 2022. Complex and flexible catabolism in Aromatoleum aromaticum pCyN1. Environ. Microbiol. 24, 3195–3211. https://doi.org/10.1111/1462-2920.16074.

Biegert, T., Fuchs, G., Heider, F., 1996. Evidence that anaerobic oxidation of toluene in the denitrifying bacterium *Thauera aromatica* is initiated by formation of benzylsuccinate from toluene and fumarate. Eur. J. Biochem. 238, 661–668. https://doi.org/10.1111/j.1432-1033.1996.0661w.x.

Chaumeil, P.A., Mussig, A.J., Hugenholtz, P., Parks, D.H., 2020. GTDB-Tk: a toolkit to classify genomes with the Genome Taxonomy Database. Bioinformatics 36 (6), 1925–1927. https://doi.org/10.1093/bioinformatics/btz848. March 2020.

Chen, S., Dong, X., 2005. Proteiniphilum acetatigenes gen. nov., sp. nov., from a UASB reactor treating brewery wastewater. Int. J. Syst. Evol. Microbiol. 55, 2257–2261. https://doi.org/10.1099/ijs.0.63807-0.

Coplen, T.B., Brand, W.A., Gehre, M., Groning, M., Meijer, H.A.J., Toman, B., Verkouteren, R.M., Coplen, T.B., Brand, W.A., Gröning, M., 2006. New guidelines for delta C-13 measurements. Anal. Chem. 78, 2439–2441. https://doi.org/10.1021/ac052027c.

Dorer, C., Höhener, P., Hedwig, N., Richnow, H.-H., Vogt, C., 2014. Rayleigh-based concept to tackle strong hydrogen fractionation in dual isotope analysis—the example of ethylbenzene degradation by *Aromatoleum aromaticum*. Environ. Sci. Technol. 48, 5788–5797. https://doi.org/10.1021/es404837g.

Dorer, C., Vogt, C., Neu, T.R., Stryhanyuk, H., Richnow, H.-H., 2016. Characterization of toluene and ethylbenzene biodegradation under nitrate-, iron(III)- and manganese (IV)-reducing conditions by compound-specific isotope analysis. Environ. Pollut. 211, 271–281. https://doi.org/10.1016/j.envpol.2015.12.029.

Evans, P.J., Mang, D.T., Kim, K.S., Young, L.Y., 1991. Anaerobic degradation of toluene by a denitrifying bacterium. Appl. Environ. Microbiol. 57, 1139–1145.

Elsner, M., 2010. Stable isotope fractionation to investigate natural transformation mechanisms of organic contaminants: principles, prospects and limitations. J. Environ. Monit. 12, 2005. https://doi.org/10.1039/c0em00277a.

Elsner, M., Zwank, L., Hunkeler, D., Schwarzenbach, R.P., 2005. A new concept linking observable stable isotope fractionation to transformation pathways of organic pollutants. Environ. Sci. Technol. 39, 6896–6916. https://doi.org/10.1021/es0504587.

Filley, C.M., Halliday, W., Kleinschmidt-DeMasters, B.K., 2004. The effects of toluene on the central nervous system. J. Neuropathol. Exp. Neurol. 63, 1–12. https://doi.org/10.1093/jnen/63.1.1.

Fischer, A., Herklotz, I., Herrmann, S., Thullner, M., Weelink, S.A.B., Stams, A.J.M., Schlömann, M., Richnow, H.-H., Vogt, C., 2008. Combined carbon and hydrogen isotope fractionation investigations for elucidating benzene biodegradation pathways. Environ. Sci. Technol. 42, 4356–4363. https://doi.org/10.1021/es702468f.

Heider, J., Szaleniec, M., Martins, B.M., Seyhan, D., Buckel, W., Golding, B.T., 2016. Structure and function of benzylsuccinate synthase and related fumarate-adding glycyl radical enzymes. Microb. Physiol. 26, 29–44. https://doi.org/10.1159/000441656.

Huskey, W, 1991. Origins and interpretations of heavy-atom isotope effects. In: Paul, F. (Ed.), Enzyme mechanism from isotope effects. CRC Press, pp. 37–72.

Jain, C., Rodriguez-R, L.M., Phillippy, A.M., Konstantinidis, K.T., Aluru, S., 2018. High throughput ANI analysis of 90K prokaryotic genomes reveals clear species boundaries. Nat. Commun. 9, 5114. https://doi.org/10.1038/s41467-018-07641-9.

Kim, D.-J., Park, M.-R., Lim, D.-S., Choi, J.-W., 2013. Impact of nitrate dose on toluene degradation under denitrifying condition. Appl. Biochem. Biotechnol. 170, 248–256. https://doi.org/10.1007/s12010-013-0176-4.

Klindworth, A., Pruesse, E., Schweer, T., Peplies, J., Quast, C., Horn, M., Glöckner, F.O., 2013. Evaluation of general 16S ribosomal RNA gene PCR primers for classical and next-generation sequencing-based diversity studies. Nucleic Acids Res. 41, e1. https://doi.org/10.1093/nar/gks808.

Kümmel, S., Kuntze, K., Vogt, C., Boll, M., Heider, J., Richnow, H.H., 2013. Evidence for benzylsuccinate synthase subtypes obtained by using stable isotope tools. J. Bacteriol. 195, 4660–4667. https://doi.org/10.1128/JB.00477-13.

Long, A., Zhang, H., Lei, Y., 2013. Surfactant flushing remediation of toluene contaminated soil: optimization with response surface methodology and surfactant recovery by selective oxidation with sulfate radicals. Separ. Purif. Technol. 118, 612–619. https://doi.org/10.1016/j.seppur.2013.08.001.

Meckenstock, R.U., Morasch, B., Warthmann, R., Schink, B., Annweiler, E., Michaelis, W., Richnow, H.H., 1999. 13C/12C isotope fractionation of aromatic hydrocarbons during microbial degradation. Environ. Microbiol. 1, 409–414. https://doi.org/10.1046/j.1462-2920.1999.00050.x.

Mukherjee, P., Roy, P., 2013. Persistent organic pollutants induced protein expression and immunocrossreactivity by *Stenotrophomonas maltophilia* PM102: a prospective bioremediating candidate. BioMed Res. Int. 2013, e714232 https://doi.org/10.1155/2013/714232.

Müller, S., Vogt, C., Laube, M., Harms, H., Kleinsteuber, S., 2009. Community dynamics within a bacterial consortium during growth on toluene under sulfate-reducing conditions. FEMS (Fed. Eur. Microbiol. Soc.) Microbiol. Ecol. 70, 586–596. https://doi.org/10.1111/j.1574-6941.2009.00768.x.

Ojeda, A.S., Phillips, E., Mancini, S.A., Lollar, B.S., 2019. Sources of uncertainty in biotransformation mechanistic interpretations and remediation studies using CSIA. Anal. Chem. 91, 9147–9153. https://doi.org/10.1021/acs.analchem.9b01756.

Oosterkamp, M.J., Veuskens, T., Saia, F.T., Weelink, S.A.B., Goodwin, L.A., Daligault, H. E., et al., 2013. Genome analysis and physiological comparison of Alicycliphilus denitrificans strains BC and K601T. PLoS One 8, e66971. https://doi.org/10.1371/journal.pone.0066971.

Parks, D.H., Imelfort, M., Skennerton, C.T., Hugenholtz, P., Tyson, G.W., 2015. CheckM: assessing the quality of microbial genomes recovered from isolates, single cells, and metagenomes. Genome Res. 25, 1043–1055. https://doi.org/10.1101/gr.186072.114.

Rabus, R., Wöhlbrand, L., Thies, D., Meyer, M., Reinhold-Hurek, B., Kämpfer, P., 2019. Aromatoleum gen. nov., a novel genus accommodating the phylogenetic lineage including Azoarcus evansii and related species, and proposal of Aromatoleum aromaticum sp. nov., Aromatoleum petrolei sp. nov., Aromatoleum bremense sp. nov., Aromatoleum toluolicum sp. nov. and Aromatoleum diolicum sp. nov. Int. J. Syst. Evol. Microbiol. 69, 982–997. https://doi.org/10.1099/ijsem.0.003244.

Rabus, R., Trautwein, K., Wöhlbrand, L., 2014. Towards habitat-oriented systems biology of “Aromatoleum aromaticum” EbN1: chemical sensing, catabolic network modulation and growth control in anaerobic aromatic compound degradation. Appl. Microbiol. Biotechnol. 98, 3371–3388. https://doi.org/10.1007/s00253-013-5466-9.

Rajamanickam, R., Kaliyamoorthi, K., Ramachandran, N., Baskaran, D., Krishnan, J., 2017. Batch biodegradation of toluene by mixed microbial consortia and its kinetics. International Biodeterioration & Biodegradation. Environmental Biotechnologies for Sustainable Development (EBSuD) 119, 282–288. https://doi.org/10.1016/j.ibiod.2016.11.014.

Richter, M., Rosselló-Móra, R., Oliver Glöckner, F., Peplies, J., 2016. JSpeciesWS: a web server for prokaryotic species circumscription based on pairwise genome comparison. Bioinformatics 32, 929–931. https://doi.org/10.1093/bioinformatics/btv681.

Ridgway, H.F., Safarik, J., Phipps, D., Carl, P., Clark, D., 1990. Identification and catabolic activity of well-derived gasoline-degrading bacteria from a contaminated aquifer. Appl. Environ. Microbiol. 56 (11), 3565–3575. https://doi.org/10.1128/aem.56.11.3565-3575.1990.

Schubert, M., Lindgreen, S., Orlando, L., 2016. AdapterRemoval v2: rapid adapter trimming, identification, and read merging. BioMed Central Research Notes 9, 1–7. https://doi.org/10.1186/s13104-016-1900-2.

Smith, T.F., Waterman, M.S., 1981. Identification of common molecular subsequences. J. Mol. Biol. 147, 195–197. https://doi.org/10.1016/0022-2836(81)90087-5.

Solano, F.M., Marchesi, M., Thomson, N.R., Bouchard, D., Aravena, R., 2018. Carbon and hydrogen isotope fractionation of benzene, toluene, and o-xylene during chemical oxidation by persulfate. Ground Water Monit. Remediat. 38, 62–72. https://doi.org/10.1111/gwmr.12228.

Solís-González, C.J., Loza-Tavera, H., 2019. *Alicycliphilus* : current knowledge and potential for bioremediation of xenobiotics. J. Appl. Microbiol. 126, 1643–1656. https://doi.org/10.1111/jam.14207.

Tan, W.A., Parales, R.E., 2019. Hydrocarbon degradation by betaproteobacteria. In: McGenity, T.J. (Ed.), Taxonomy, Genomics and Ecophysiology of Hydrocarbon-Degrading Microbes. Springer International Publishing, Cham, pp. 125–141. https://doi.org/10.1007/978-3-030-14796-9_18.

Ueki, A., Akasaka, H., Suzuki, D., Ueki, K., 2006. Paludibacter propionicigenes gen. nov., sp. nov., a novel strictly anaerobic, Gram-negative, propionate-producing bacterium isolated from plant residue in irrigated rice-field soil in Japan. Int. J. Syst. Evol. Microbiol. 56, 39–44. https://doi.org/10.1099/ijs.0.63896-0.

Vallenet, D., Calteau, A., Dubois, M., Amours, P., Bazin, A., Beuvin, M., et al., 2020. MicroScope: an integrated platform for the annotation and exploration of microbial gene functions through genomic, pangenomic and metabolic comparative analysis. Nucleic Acid Res 48, D579–D589. https://doi.org/10.1093/nar/gkz926.

Vogt, C., Cyrus, E., Herklotz, I., Schlosser, D., Bahr, A., Herrmann, S., Richnow, H.-H., Fischer, A., 2008. Evaluation of toluene degradation pathways by two-dimensional stable isotope fractionation. Environ. Sci. Technol. 42, 7793–7800. https://doi.org/10.1021/es8003415.

Wartell, B., Boufadel, M., Rodriguez-Freire, L., 2021. An effort to understand and improve the anaerobic biodegradation of petroleum hydrocarbons: a literature review. Int. Biodeterior. Biodegrad. 157, 105156 https://doi.org/10.1016/j.ibiod.2020.105156.

Weelink, S.A.B., Van Doesburg, W., Saia, F.T., Rijpstra, W.I.C., Röling, W.F.M., Smidt, H., Stams, A.J.M., 2009. A strictly anaerobic betaproteobacterium *Georgfuchsia toluolica* gen. nov., sp. nov. degrades aromatic compounds with Fe(III), Mn(IV) or nitrate as an electron acceptor. FEMS (Fed. Eur. Microbiol. Soc.) Microbiol. Ecol. 70, 575–585. https://doi.org/10.1111/j.1574-6941.2009.00778.x.

Weelink, S.A.B., van Eekert, M.H.A., Stams, A.J.M., 2010. Degradation of BTEX by anaerobic bacteria: physiology and application. Rev. Environ. Sci. Biotechnol. 9, 359–385. https://doi.org/10.1007/s11157-010-9219-2.

Weiten, A., Kalvelage, K., Becker, P., Reinhardt, R., Hurek, T., Reinhold-Hurek, B., Rabus, R., 2021. Complete genomes of the anaerobic degradation specialists *Aromatoleum petrolei* ToN1^{T} and *Aromatoleum bremense* PbN1^{T}. Microb. Physiol. 31, 16–35. https://doi.org/10.1159/000513167.

Wijker, R.S., Adamczyk, P., Bolotin, J., Paneth, P., 2013. Isotopic analysis of oxidative pollutant degradation pathways exhibiting large H isotope fractionation. Environ. Sci. Technol. 47, 13459–13468. https://doi.org/10.1021/es403597v.

Zhang, N., Geronimo, I., Paneth, P., Schindelka, J., Schaefer, T., Herrmann, H., Vogt, C., 2016. Analyzing sites of OH radical attack (ring vs. side chain) in oxidation of substituted benzenes via dual stable isotope analysis (δ13C and δ2H). Sci. Total Environ. 542, 484–494. https://doi.org/10.1016/j.scitotenv.2015.10.075.

Zhu, B., Friedrich, S., Wang, Z., Táncsics, A., Lueders, T., 2020. Availability of nitrite and nitrate as electron acceptors modulates anaerobic toluene-degrading communities in aquifer sediments. Front. Microbiol. 11, 1867. https://doi.org/10.3389/fmicb.2020.01867.